Supporting Information

Creating Nitrogen Doped Hollow Multi-yolk@Shell Carbon as High Performance Electrodes for Flow-through Deionization Capacitors

Hui Wang, [†,‡] Tingting Yan, [†] Liyi Shi, [†] Guorong Chen, [†] Jianping Zhang, [†] Dengsong Zhang[†]*

[†]Research Center of Nano Science and Technology, Shanghai University, Shanghai, 200444 (P. R. China)

[‡]School of Environmental Science and Engineering, Yancheng Institute of Technology, Jiangsu, 224000 (P. R. China)

Corresponding author: E-mail: dszhang@shu.edu.cn

Number of pages: 11

Number of figures: 9

Number of tables:2

Supporting Information content

Figure S1 XRD patterns of HC.

Figure S2 Raman spectrum of HC.

Figure S3 XPS spectrum of HMYSC.

Figure S4 Plots of water contact angles on different carbon electrodes *versus* contact time.

Figure S5 CV profiles of the HMYSC and HC electrodes at 1 mVs^{-1} in a 0.009 M (500 mg L^{-1}) NaCl solution.

Figure S6 CV profiles of the HMYSC, HC, YSC-1, YSC-2 and N-doped C electrodes at 10 mVs^{-1} in a 0.5 M NaCl solution.

Figure S7 FTDC profiles of HMYSC electrode in a 500 mg L^{-1} NaCl solution with a flow rate of 30mL min^{-1} at a working voltage of 1.2 V.

Figure S8 Current transient for HC and HMYSC electrodes in a NaCl solution with a concentration of 500 mg L^{-1} at a working voltage of 1.4 V.

Figure S9 Electrosorption comparison of HC and HMYSC electrodes under different voltage in a NaCl solution with a concentration of 100 mg L^{-1}.

Table S1 Detailed specific surface and pore volume data of the HMYSC and HC.

Table S2 Comparison of the FTDC performance among different carbon-based electrodes reported in the literatures.

Experimental section

Preparation of the HC

Monodisperse SiO_2 microspheres were prepared according to the previously reported method for the following use.[1] For RF coating, 0.8 g of as-obtained SiO_2 spheres was firstly dispersed in deionized water (DI, 70.4 mL) by sonication, and then 2.3 g of CTAB, 0.35 g of resorcinol, 28.2 mL of ethanol and 0.1 mL of ammonia were added into above SiO_2 dispersion, and stirring at 35 °C for 30 min to form a uniform dispersion. Then, 0.5 mL of a formalin solution was added to the dispersion under stirring. After 6 h continuous stirring, the mixture was cooled to room temperature, and then aged at room temperature overnight. The product RF@SiO_2 was collected by centrifugation and then washed with the deionization water and ethanol several times. The carbonization of the RF@SiO_2 was completed at 400 °C for 2 h and 800 °C for 2 h under a N_2 atmosphere with a heating rate of $1°C$ min^{-1}. The obtained silica–carbon composite was further treated with a 10 wt% HF aqueous solution to remove the silica template completely, followed by washing with plenty of DI water, and drying at 60 °C for 24 h. The resultant sample was denoted as HC.

Preparation of the nitrogen-doped carbon (N-doped C)

For polydopamine (PDA) coating, 0.24 g monodisperse SiO_2 microspheres was dispersed in 75 mL 10 mM Tris solution (Ph=8.6) through sonication, and then 0.24 g dopamine was added under continiously striring. After reacting 24 h, the PDA@SiO_2 was collected by vacume filtration and wased by DI water and ethnol for several times. The carbonization of the PDA@SiO_2 was completed at 400 °C for 2 h and 800 °C for 2 h under a N_2 atmosphere with a heating rate of $1°C$ min^{-1}. The obtained silica–carbon composite was further treated with a 10 wt% HF aqueous solution to remove the silica template completely, followed by washing with plenty of DI water, and drying at 60 °C for 24 h. The resultant sample was denoted as **N-doped C**.

Preparation of the mSiO₂@RF@SiO₂ with different amount of TEOS

0.1 g RF@SiO$_2$, 0.16 g CTAB and 1.5 mL ammonia were added into the mixture solution of ethanol and DI water (v/v=4:1), after sonication for 1h, (0.94-1.24 g) TEOS diluted by ethanol was added drop by drop, and then stirred 12 h. The resulted mSiO$_2$@RF@SiO$_2$ was collected by vacuum filtration and then washed with ethanol several times. The mSiO$_2$@RF@SiO$_2$ was dried at 60 ^{o}C overnight. The next PDA coating and HF etching process is same as the HMYSC. The resulted sample with different TEOS amount was denoted YSC-1and YSC-2.
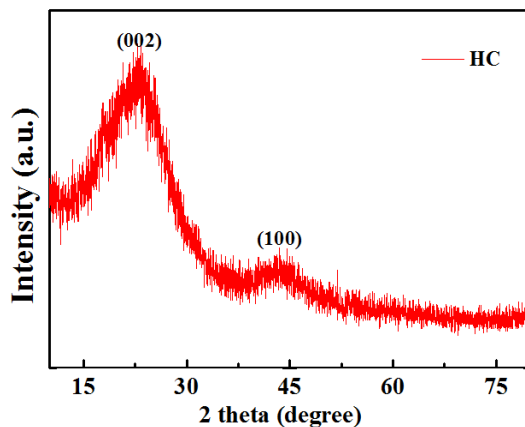
Results and discussion
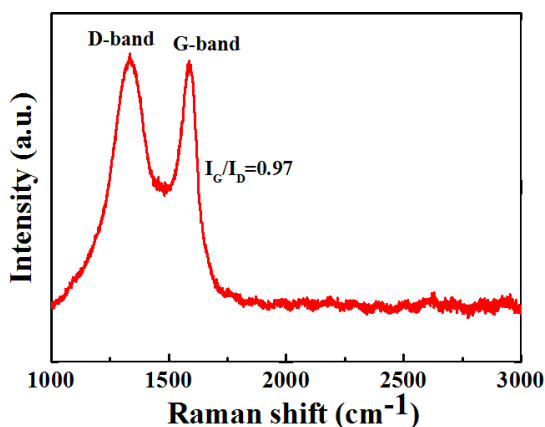

Figure S1 XRD patterns of HC

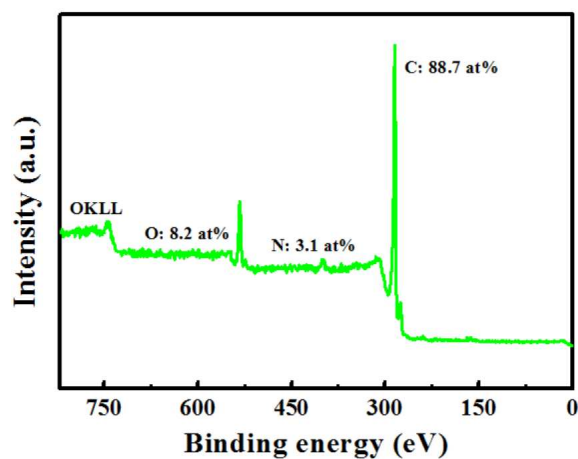**Figure S2** Raman spectrum of HC.

Figure S3 XPS spectrum of HMYSC.

The full XPS spectrum of HMYSC is shown in Figure S3. The nitrogen content of HMYSC is 3.1 at%. No obvious peak of Si is detected, suggesting the effective removal of Si species of HMYSC due to completely etching by HF. Besides, the F species also cannot be observed during the XPS analysis. Therefore, HMYC is a pure N-doped carbon material.
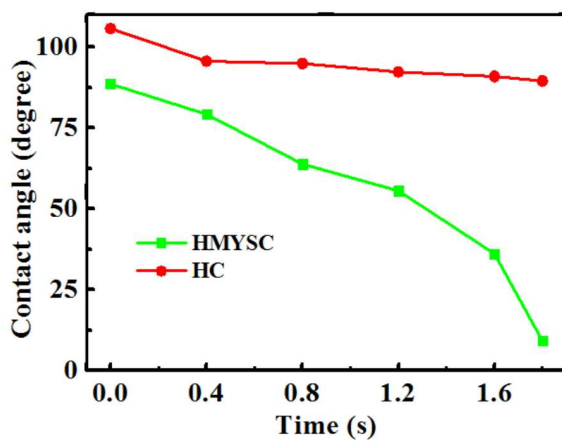

Figure S4 Plots of water contact angles on different carbon electrodes *versus* contact time.
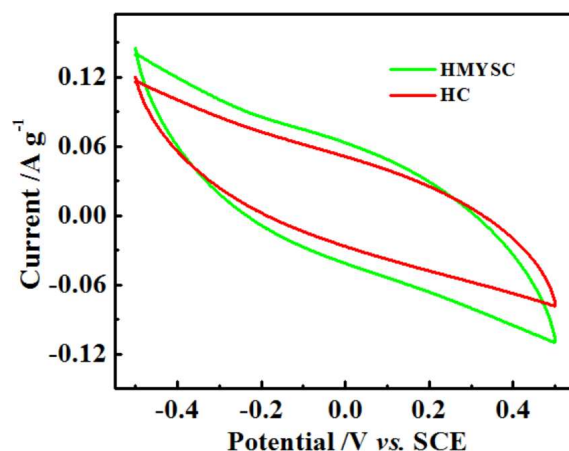
Figure S5 CV profiles of the HMYSC and HC electrodes at 1 mVs^{-1} in a 0.009 M (500 mg L^{-1}) NaCl solution.
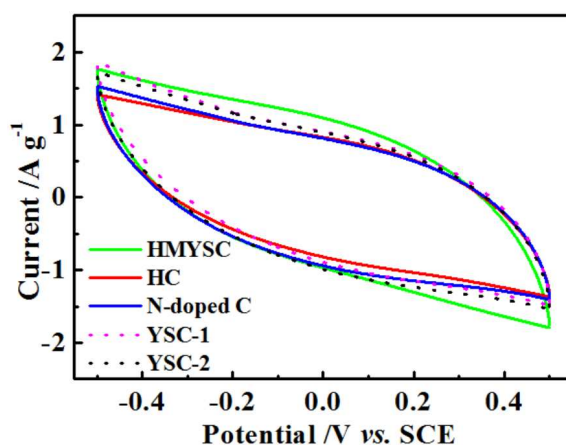

Figure S6 CV profiles of the HMYSC, HC, YSC-1, YSC-2 and N-doped C electrodes at 10 mVs^{-1} in a 0.5 M NaCl solution.

The CV curves of HMYSC, HC, YSC-1, YSC-2 and N-doped C electrodes in a 0.5 M NaCl solution is shown in Figure S6. The CV curves present a leaf-like shape instead of rectangular-like structure due to higher scan rate. It should be noted that the CV curve area of HMYSC electrode is larger than that of N-doped C, suggesting the higher specific capacitance of HMYSC electrodes due to multi-yolk structure of HMYSC providing more adsorption sites. The HMYSC electrode also shows larger area of CV curve than the HC, YSC-1 and YSC-2, because the HMYSC has a larger surface area and a higher pore volume, which is beneficial to salt ion accumulation and adsorption.

Therefore, combining hierarchically porous structure, larger surface area and higher pore volume, the HMYSC is more suitable to high performance capacitive deionization.
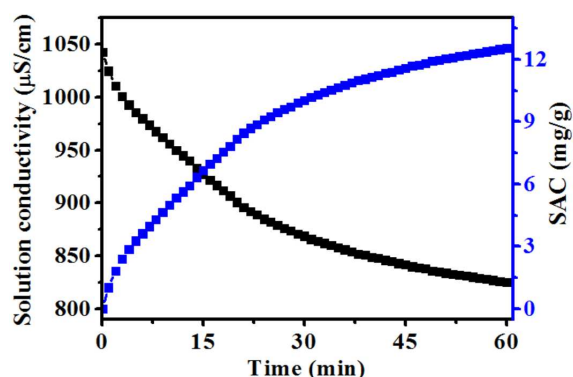

Figure S7 FTDC profiles of HMYSC electrode in a 500 mg L^{-1} NaCl solution with a flow rate of 30mL min^{-1} at a working voltage of 1.2 V.

The electrosorption performance of the HMYSC electrode in NaCl solution with high initial conductivity was also investigated in this work. Figure S7 presents the desalination curve in NaCl solution with an initial conductivity of 1050 μS cm^{-1} at a working voltage of 1.2 V. At first, the conductivity dramatically decreased and then becomes stable after about 60 minutes. The electrosorption capacity of the HMYSC electrode is 12.6 mg g^{-1} according to eqn (1).
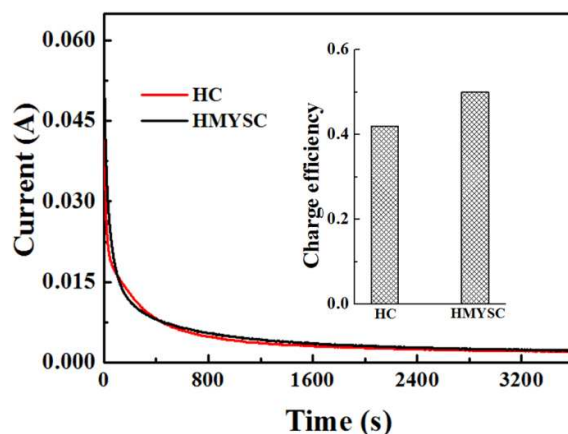
Figure S8 Current transient for HC and HMYSC electrodes in a NaCl solution with a concentration of 500 mg L^{-1} at a working voltage of 1.4 V.

Charge efficiency (Λ) is a crucially important parameter to evaluate the double layer formed at the interface between the electrode and solution, as described according to the following equation:

$$\Lambda=\Gamma\times F/\Sigma$$

where F is the Faraday constant (96485 C mol^{-1}), Γ is the electrosorption capacity (mol g^{-1})and Σ (charge, C g^{-1}) is obtained by integrating the corresponding current. The current response curves are shown in Figure S8. As calculated, the charge efficiency of HMYSC is 0.50, a bit larger than that of HC (0.43). The charge efficiency of electrodes is always below 1.0, which is ascribed to the following reasons: (i) The binder used during the electrode fabrication process can decrease the conductivity and surface area of the electrode materials. (ii) The weak adhesion between current collector and porous electrode may lead to lower charge efficiency.[2] (iii) The co-ions expelled from the EDL when the counter-ion are adsorbed onto the electrodes.[2, 3] It is noted that the charge efficiency can be further improved by using a charge barrier membrane into FTDC in the practical use. [4, 5]
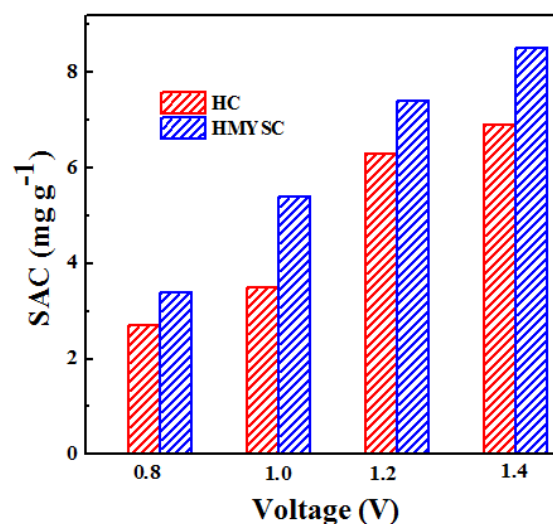
Figure S9 Electrosorption comparison of HC and HMYSC electrodes under different voltage in a NaCl solution with a concentration of 100 mg L^{-1}.

Table S1 Detailed specific surface and pore volume data of the HMYSC and HC.

Sample	Specific surface area (m^2 g^{-1})			Pore Volume (mL g^{-1})		
	S_{BET}	S_{ext}	S_{mic}	Micropore	Mesopore	Total
HMYSC	910	641	269	0.13	3.36	3.49
HCS	534	185	349	0.15	2.35	2.50

Table S2 Comparison of the FTDC performance among different carbon-based electrodes reported in the literatures.

Electrode material	Applied voltage (V)	Initial concentration (mg L^{-1})	Deionization Time (min)	SAC (mg g^{-1})	Ref.
AC	1.2	500	180	9.7	6
AC	1.2	500	180	5.5	7
GR	2.0	250	100	4.6	8
CNTs	1.2	1000	200	3.7	9
CNTs	1.2	500	40	2.8	10
CNFs	1.6	95	150	4.6	11
CA	1.3	2000	-	7.1	12
PC	1.2	500	180	9.1	7
PCS	1.6	500	40	5.8	10
CNFs-RGO	1.2	400	40	7.2	13
RG-AC	1.2	500	60	2.9	14
bc-CNFs	1.2	500	40	10.7	15
HMYSC	1.2	500	60	12.6	This work
HMYSC	1.2	500	40	11.2	This work
HMYSC	1.4	500	60	16.1	This work
HMYSC	1.4	300	60	14.2	This work

References

(1) Wen, X. R.; Zhang, D. S.; Shi, L. Y.; Yan, T. T.; Wang, H.; Zhang, J. P., Three-dimensional hierarchical porous carbon with a bimodal pore arrangement for capacitive deionization. *J. Mater. Chem.* **2012**, 22, 23835–23844.

(2) Liu, Y.; Xu, X.; Wang, M.; Lu, T.; Sun, Z.; Pan, L., Metal-organic framework-derived porous carbon polyhedra for highly efficient capacitive deionization. *Chem. Commun.* **2015**, 51, 12020-3.

(3) Andelman, M., Ionic group derivitized nano porous carbon electrodes for capacitive deionization. *J. Mater. Sci. Chem. Eng.* **2014**, 02, 16-22.

(4) Zhao, R.; Satpradit, O.; Rijnaarts, H. H.; Biesheuvel, P. M.; van der Wal, A., Optimization of salt adsorption rate in membrane capacitive deionization. *Water Res.* **2013**, 47, 1941-52.

(5) Liu, Y.; Pan, L.; Xu, X.; Lu, T.; Sun, Z.; Chua, D. H. C., Enhanced desalination efficiency in modified membrane capacitive deionization by introducing ion-exchange polymers in carbon nanotubes electrodes. *Electrochim. Acta* **2014**, 130, 619-624.

(6) Chen, Z.; Song, C.; Sun, X.; Guo, H.; Zhu, G., Kinetic and isotherm studies on the electrosorption of NaCl from aqueous solutions by activated carbon electrodes. *Desalination* **2011**, 267, 239-243.

(7) Chang, L.; Li, J.; Duan, X.; Liu, W., Porous carbon derived from Metal–organic framework (MOF) for capacitive deionization electrode. *Electrochim. Acta* **2015**, 176, 956-964.

(8) Jia, B. P., Zhou L., Wettability and its influence on graphene nansoheets as electrode material for capacitive deionization. *Chem. Phys. Lett.* **2012**, 548 23-28.

(9) Wang, S.; Wang, D. Z.; Ji, L. J.; Gong, Q. M.; Zhu, Y. F.; Liang, J., Equilibrium and kinetic studies on the removal of NaCl from aqueous solutions by electrosorption on carbon nanotube electrodes. *Sep. Purif. Technol.* **2007**, 58, 12-16.

(10) Liu, Y.; Pan, L.; Chen, T.; Xu, X.; Lu, T.; Sun, Z.; Chua, D. H. C., Porous carbon spheres via microwave-assisted synthesis for capacitive deionization. *Electrochim. Acta* **2015**, 151, 489-496.

(11) Wang, G., Pan, C., Wang, L. P., Dong, Q., Yu, C., Zhao, Z. B., Qiu, J. S., Activated carbon nanofiber webs made by electrospinning for capacitive deionization. *Electrochim. Acta* **2012**, 69 65-70.

(12) Xu, P.; Drewes, J. E.; Heil, D.; Wang, G., Treatment of brackish produced water using carbon aerogel-based capacitive deionization technology. *Water Res.* **2008**, 42, 2605-2617.

(13) Dong, Q., Wang, G., Qian, B. Q., Hu, C., Wang, Y. W., Qiu J. S., Electrospun composites made of reduced graphene oxide and activated carbon nanofibers for capacitive deionization. *Electrochim. Acta* **2014**, 137, 388-394.

(14) Li, H. B.; Pan, L. K.; Nie, C. Y.; Liu, Y.; Sun, Z., Reduced graphene oxide and activated carbon composites for capacitive deionization. *J. Mater. Chem.* **2012**, 22, 15556-155561.

(15) Liu, Y.; Lu, T.; Sun, Z.; Chu, D. H. C.; Pan, L. K., Ultra-thin carbon nanofiber networks derived from bacterial cellulose for capacitive deionization. *J. Mater. Chem. A* **2015**, 3, 8693-8700.